EPJ manuscript No.
(will be inserted by the editor)

Scalar-isovector $K\bar{K}$ production close to threshold

A. Dzyuba[1,2], V. Kleber[3a], M. Büscher[2b], V.P. Chernyshev[4c], S. Dymov[5], P. Fedorets[2,4], V. Grishina[6], C. Hanhart[2], M. Hartmann[2], V. Hejny[2], L. Kondratyuk[5], V. Koptev[1], P. Kulessa[7], Y. Maeda[2,3d], T. Mersmann[8], S. Mikirtychyants[1], M. Nekipelov[1,2], D. Prasuhn[2], R. Schleichert[2], A. Sibirtsev[2,9], H.J. Stein[2], H. Ströher[2], and I. Zychor[10]

[1] High Energy Physics Department, Petersburg Nuclear Physics Institute, 188350 Gatchina, Russia
[2] Institut für Kernphysik, Forschungszentrum Jülich, 52425 Jülich, Germany
[3] Institut für Kernphysik, Universität zu Köln, 50937 Köln, Germany
[4] Institute for Theoretical and Experimental Physics, Bolshaya Cheremushkinskaya 25, 117218 Moscow, Russia
[5] Laboratory of Nuclear Problems, Joint Institute for Nuclear Research, 141980 Dubna, Russia
[6] Institute for Nuclear Research, 60th October Anniversary Prospect 7A, 117312 Moscow, Russia
[7] Institute of Nuclear Physics, Radzikowskiego 152, 31342 Cracow, Poland
[8] Institut für Kernphysik, Universität Münster, 48149 Münster, Germany
[9] Helmholtz-Institut für Strahlen- und Kernphysik (Theorie), Universität Bonn, Nußallee 14-16, 53115 Bonn, Germany
[10] The Andrzej Sołtan Institute for Nuclear Studies, 05400 Świerk, Poland

Received: date / Revised version: date

Abstract. The reaction $pp{\to}dK^+\bar{K^0}$ has been investigated at excess energies Q= 47.4 and 104.7 MeV above the $K^+\bar{K^0}$ threshold at COSY-Jülich. Coincident dK^+ pairs were detected with the ANKE spectrometer, and subsequently $\sim$ 2000 events with a missing $\bar{K^0}$ invariant-mass were identified, which fully populate the Dalitz plot. The joint analysis of invariant-mass and angular distributions reveals s-wave dominance between the two kaons, in conjunction with a p-wave between the deuteron and the kaon pair, *i.e.* $K\bar{K}$ production via the $a_0^+(980)$ channel. Integration of the differential distributions yields total cross sections of $\sigma(pp{\to}dK^+\bar{K^0})$=$(38{\pm}2_{\rm stat}{\pm}14_{\rm syst})$ nb and $(190{\pm}4_{\rm stat}{\pm}39_{\rm syst})$ nb for the low and high Q value, respectively.

PACS. 25.10.+s Nuclear reactions involving few-nucleon systems – 13.75.-n Hadron-induced low- and intermediate-energy reactions and scattering (energy $\leq$ 10 GeV)

1 Introduction

QCD is the fundamental theory of Strong Interactions. How quarks and gluons are bound into hadrons is as yet an unsolved strong-coupling problem. Though QCD can be treated explicitly in this regime using lattice techniques [1], these are not in a state to make quantitative statements about the light scalar mesons. Alternatively, QCD-inspired models, which employ effective degrees of freedom, can be used. The constituent quark model is one of the most successful in this respect (see *e.g.* Ref. [2]). This approach inherently treats the lightest scalar resonances $a_0/f_0(980)$ as conventional $q\bar{q}$ states.

Experimentally more states with quantum numbers J^P=0^+ have been identified than would fit into a single SU(3) scalar nonet: the $f_0(600)$ (or σ), $f_0(980)$, $f_0(1370)$, $f_0(1500)$ and $f_0(1710)$ with I=0, the putative $\kappa(800)$ and the $K^*(1430)$ (I=1/2), as well as the $a_0(980)$ and $a_0(1450)$ (I=1) [3]. Consequently, the $a_0/f_0(980)$ have been associated with crypto-exotic states like $K\bar{K}$ molecules [4] or compact qq-$\bar{q}\bar{q}$ states [5]. It has even been suggested that a complete nonet of four-quark states might exist with masses below 1.0 GeV/c^2 [6].

The first clear observation of the isovector $a_0(980)$ resonance was achieved in K^-p interactions [7]. It has also been seen in $p\bar{p}$ annihilations [8], in π^-p collisions [9], and in $\gamma\gamma$ interactions [10]. Experiments on radiative ϕ-decays [11,12] have been analysed in terms of a_0/f_0 production in the decay chain $\phi \to \gamma a_0/f_0 \to \gamma\pi^0\eta/\pi^0\pi^0$. In pp collisions the $a_0(980)$ resonance has been measured at p_p = 450 GeV/c *via* $f_1(1285) \to a_0^{\pm}\pi^{\mp}$ decays [13] and in inclusive measurements of the $pp \to dX^+$ reaction at p_p = 3.8, 4.5, and 6.3 GeV/c [14].

[a] *Present address:* Physikalisches Institut, Universität Bonn, Nussallee 12, 53115 Bonn, Germany
[b] *m.buescher@fz-juelich.de*
[c] deceased
[d] *Present address:* Research Center for Nuclear Physics, Osaka University, Ibaraki, Osaka 567-0047, Japan

Despite these many experimental investigations, basic properties and even the nature of the $a_0(980)$ resonance are still far from being established (see *e.g.* Refs. [15,16]). The Particle Data Group quotes a mass of $m_{a_0} = (984.7 \pm 1.2)$ MeV/c^2 and a width of $\Gamma_{a_0} = (50 - 100)$ MeV/c^2 [3]. The main decay channels, $\pi\eta$ and $K\bar{K}$, are denoted as "dominant" and "seen", respectively. The corresponding coupling constants $g_{\pi\eta}$ and $g_{K\bar{K}}$ differ significantly for the different data sets and analyses [16].

Therefore, an experimental programme has been started at the Cooler Synchrotron COSY-Jülich [17] aimed at exclusive data on the $a_0/f_0(980)$ production from pp, pn, pd and dd interactions at energies close to the $K\bar{K}$ threshold [18]. The final goal of these investigations is the extraction of the a_0/f_0-mixing amplitude, a quantity which is believed to shed light on the nature of these resonances [19, 20]. As a first step the reactions $pp \to dK^+\bar{K^0}$ [21] and $pp \to d\pi^+\eta$ [22] have been measured in parallel at the ANKE spectrometer [23] for T_p=2.65 GeV, corresponding to an excess energy of Q=47.4 MeV with respect to the $K^+\bar{K^0}$ threshold. The data for the strangeness decay channel — which are almost background free — indicate that more than 80% of the kaon pairs are produced in a relative s-wave, corresponding to the a_0^+ channel [21]. On the other hand, the $\pi^+\eta$ signal sits on top of a strong but smooth background of multi-pion production which, together with the small acceptance of ANKE for this channel, makes the interpretation of the a_0^+ signal model-dependent [22]. However, the obtained branching ratio $\sigma(pp{\to}d(K^+\bar{K^0})_{s-\mathrm{wave}})/\sigma(pp{\to}da_0^+{\to}d\pi^+\eta) = 0.029 \pm 0.008_{\mathrm{stat}} \pm 0.009_{\mathrm{sys}}$ [22] is in line with values from literature [3].

In this paper we report on a refined analysis of the $pp \to dK^+\bar{K^0}$ data at T_p=2.65 GeV as well as on new results from a second measurement at higher beam energy (T_p = 2.83 GeV, corresponding to Q = 104.7 MeV). The procedures for event identification and acceptance correction at the lower energy have been described in our previous publication [21].

2 Measurement of pp $\longrightarrow$ dK$^+\bar{\mathrm{K}}^0$ events with ANKE

2.1 Experimental setup

ANKE is a magnetic spectrometer located in one of the straight sections of COSY and comprises three dipole magnets, D1 – D3 [23]. D1 deflects the circulating COSY beam onto the target in front of D2, and D3 bends it back into the nominal orbit. The C-shaped spectrometer dipole D2 separates forward-going reaction products from the COSY beam and allows one to determine their emission angles and momenta. The angular acceptance of ANKE covers $|\vartheta_{\mathrm{h}}| \leq 10^\circ$ horizontally and $|\vartheta_{\mathrm{v}}| \leq 3^\circ$ vertically for the detected deuterons ($p_d > 1300$ MeV/c), and $|\vartheta_h| \leq 12^\circ$ and $|\vartheta_v| \leq 3.5^\circ$ for the K^+ mesons.

A cluster-jet target [24] of hydrogen molecules, placed between D1 and D2, has been used, providing areal densities of up to $\sim 5{\times}10^{14}$ cm^{-2}. The luminosity has been measured with high statistical accuracy using pp elastic scattering, recorded simultaneously with the dK^+ data. Protons with $\vartheta = 5.5^\circ - 9^\circ$ have been selected, since the ANKE acceptance changes smoothly in this angular range and the elastic peak is easily distinguished from background in the momentum distribution. The average luminosity during the measurements with up to $\sim 4 \times 10^{10}$ stored protons in the COSY ring has been determined as $L = (1.7{\pm}0.4_{\mathrm{syst}}){\times}10^{31}\,\mathrm{s}^{-1}\,\mathrm{cm}^{-2}$, corresponding to an integrated value of $L_{\mathrm{int}} = 7.5\,\mathrm{pb}^{-1}$.

2.2 Event selection for Q = 104.7 MeV

Two charged particles, K^+ and d, have been detected in coincidence. Positively charged kaons are identified in the side detection system (SD) [23,25] of ANKE by a time-of-flight (TOF) measurement. The TOF-start counters, consisting of one layer of 23 scintillation counters, have been mounted next to the large exit window of the vacuum chamber in D2. Kaons from a_0^+ decay with momenta $p_{K^+} = 390 - 625$ MeV/c have been stopped in range telescopes, located along the focal surface of D2. These telescopes comprise TOF-stop counters and provide additional kaon-*vs*-background discrimination by means of energy-loss (ΔE) measurements [25]. At $T_p = 2.83$ GeV, kaons with $p_{K^+} = (625 - 1000)$ MeV/c have been detected in a different part of the SD, consisting of one layer of 6 scintillation counters for TOF-stop ("sidewall counters"). Two multi-wire proportional chambers (MWPCs) positioned between the TOF-start and -stop counters allow one to deduce the ejectile momenta and to suppress background from secondary scattering [21,22].

Fast particles produced in coincidence with the K^+ mesons as well as elastically scattered protons have been detected in the ANKE forward-detection system (FD) [26] containing two layers of scintillation counters for TOF and ΔE measurements. In addition there are three MWPCs, each with two sensitive planes, exploited for momentum reconstruction and background suppression [21,23]. Two bands of protons and deuterons are distinguished in the time difference between the detection of a K^+-meson in one of the TOF-stop counters of the SD and a particle in the FD as a function of the FD particle momentum, see Fig. 1a. The deuterons are selected with the cut indicated by the lines, plus the energy-loss information from the FD scintillation counters. In Fig. 1b the missing-mass distribution $m(pp, dK^+)$ for the selected $pp{\to}dK^+X$ events is presented. The missing particle X must be a $\bar{K}^0$, due to charge and strangeness conservation. The measured dK^+ missing-mass distribution peaks around $m{=}m_{\bar{K}^0}$, reflecting the clean particle identification at ANKE.

About 2300 events are accepted as $dK^+\bar{K}^0$ candidates for further analysis (unshaded peak area of the histogram in Fig. 1b)). The remaining background from misidentified particles is (13±2) %. The shape of this background in the differential spectra discussed below has been determined

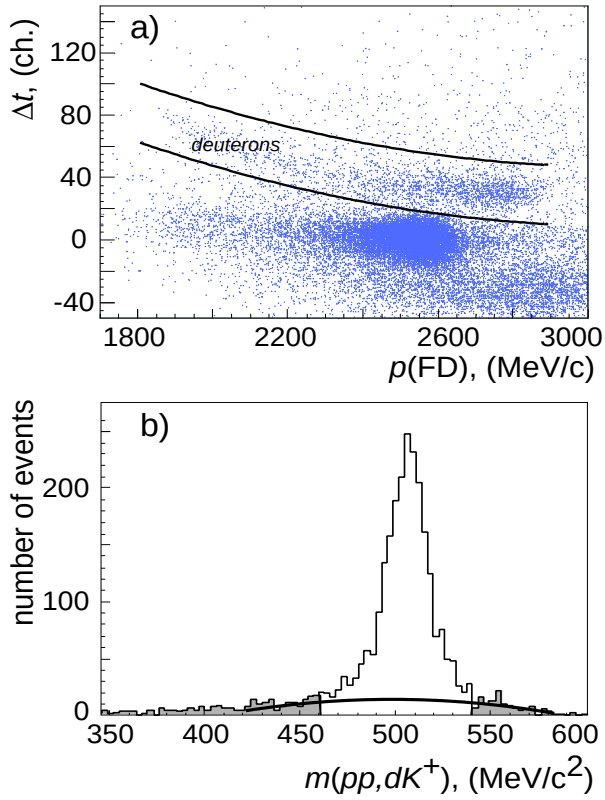

Fig. 1. a) Time difference between the fast forward-going particles in layer 1 of the FD scintillators and the K^+-mesons *vs.* the momentum of the forward particle. The lines indicate the selection for deuteron identification. b) Missing-mass $m(pp, dK^+)$ distribution of the $pp{\to}dK^+X$ events. The shaded areas indicate the events used for background subtraction, the solid line shows the background distribution under the $\bar{K}^0$ peak obtained from a polynomial fit.

and subsequently subtracted by selecting events outside the $\bar{K}^0$ peak (shaded areas in Fig. 1b).

The K^+ tracking efficiency in the side MWPCs and the efficiency of the ΔE cut have been determined using simultaneously recorded $pp{\to}pK^+\Lambda$ events, which, due to the significantly larger cross section, can be identified by TOF criteria and a momentum cut for protons in the FD only. The efficiency of the track reconstruction varies from 96% for the telescopes to 76% for the sidewall counters. The efficiency of the ΔE cut has been determined for each telescope, with an average value of 53%, and for the sidewall counters, ranging from 87% to 74%. The efficiency of the FD ΔE criterion for deuterons has been deduced from the number of $\bar{K}^0$ events in the peak of Fig. 1b before and after this cut. The efficiency of the FD scintillators and all TOF criteria is larger than 99%. The data have been corrected for all efficiencies on an event-by-event basis.

2.3 Kinematic fit

A kinematic fit has been carried out to improve the invariant-mass and angular resolutions. This fit shifts the measured dK^+ missing mass (Fig. 1b) to the nominal value of $m_{\bar{K}^0} = 497.6\,\mathrm{MeV/c^2}$ on an event-by-event basis, varying the momentum components of the detected K^+ and d within their resolutions. As a result of the fit, the deuteron missing-mass (*i.e.* the invariant $K^+\bar{K}^0$ mass) resolution improves from $\delta m_{K^+\bar{K}^0} = (35-3)\,\mathrm{MeV/c^2}$ over the range (991 – 1096) MeV/c^2 to $\delta m_{K^+\bar{K}^0} < 10\,\mathrm{MeV/c^2}$ in the full range with minimum values of $\sim 3\,\mathrm{MeV/c^2}$ at the kinematic limits. Due to the fact that the p_z resolution (z being the beam direction) for deuterons is approximately a factor five worse than for all other variables, the fit procedure does not significantly improve the K^+ missing-mass and angular resolutions: $\delta m_{d\bar{K}^0} \sim 5\,\mathrm{MeV/c^2}$ in the full range, $\delta[\cos(\theta)] \sim 0.2$ for all angular spectra.

The same fit procedure has also been applied to the previously published data at T_p =2.65 GeV [21], and improves $\delta m_{K^+\bar{K}^0}$ from (8 – 1) $\mathrm{MeV/c^2}$ over the range (991 – 1038) $\mathrm{MeV/c^2}$ to $\delta m_{K^+\bar{K}^0} < 3\,\mathrm{MeV/c^2}$ in the full mass range.

2.4 Non-acceptance-corrected Dalitz plot

Figure 2 shows the distribution of the kinematically fitted $dK^+\bar{K}^0$ events in the Dalitz plot for both Q values. It is observed that the kinematically allowed region is fully covered by the ANKE acceptance. For comparison the simulated population of the Dalitz plot is also shown for the case of phase-space-distributed events. The total ANKE acceptance for these $dK^+\bar{K}^0$ events is 2.1% at Q = 47.4 MeV and 0.8% at 104.7 MeV. Due to the limited number of counts we present in the following only one-dimensional distributions. These also have the advantage of carrying additional information about the transition matrix, as shown in Sect. 2.5.

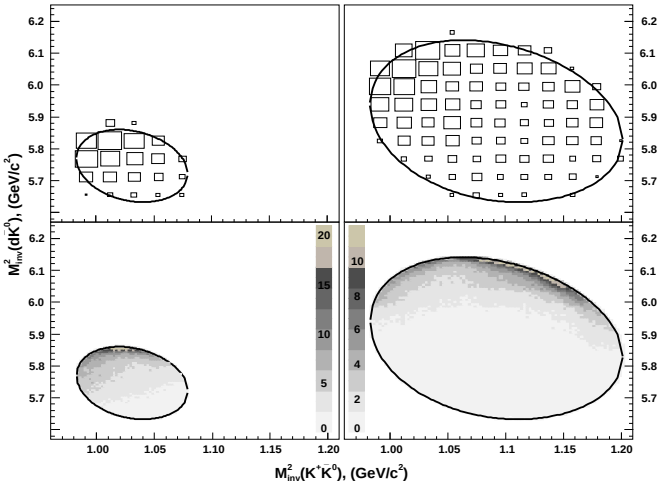

Fig. 2. Upper: Dalitz plot of the events from the reaction $pp{\to}dK^+\bar{K}^0$ at Q = 47.4 (left) and 104.7 MeV (right). The data are not background subtracted and not corrected for the ANKE acceptance and the detection efficiencies, and are binned with cell size $21\,\mathrm{MeV^2}/c^4{\times}57\,\mathrm{MeV^2}/c^4$ The lines denote the kinematically allowed region. Lower: Simulated Dalitz-plots inside the ANKE acceptance for phase-space distributed events (*i.e.* configuration $[(K\bar{K})_s d]_s$, cf. Sect. 2.5).

2.5 Acceptance correction

In comparison to the data at $T_p = 2.65$ GeV [21], the excess energy for the higher beam energy is approximitely twice as large. As a consequence, the method of model-independent acceptance correction (using a five-dimensional acceptance matrix) can no longer be used, since the number of zero elements in the acceptance matrix becomes too large. An alternative method has been developed which is described as follows.

In the close-to-threshold regime only a limited number of final states contribute. For the data analysis we have restricted ourselves to the lowest allowed partial waves, *i.e.* s-wave in the $K\bar{K}$ system accompanied by a p-wave of the deuteron with respect to the meson pair ($a_0^+(980)$-channel) and p-wave $K\bar{K}$ production with an s-wave deuteron (non-resonant channel). In the following we denote these two configurations by $[(K\bar{K})_s d]_p$ and $[(K\bar{K})_p d]_s$. It has been shown that the lower energy data can be described by this *ansatz* for the $dK^+\bar{K}^0$ final state [21], where the square of the spin-averaged transition matrix element can be written as:

$$|\bar{\mathcal{M}}|^2 = C_0^q q^2 + C_0^k k^2 + C_1(\hat{\boldsymbol{p}}\cdot\boldsymbol{k})^2 + C_2(\hat{\boldsymbol{p}}\cdot\boldsymbol{q})^2 + C_3(\boldsymbol{k}\cdot\boldsymbol{q}) + C_4(\hat{\boldsymbol{p}}\cdot\boldsymbol{k})(\hat{\boldsymbol{p}}\cdot\boldsymbol{q})\ . \quad (1)$$

Here $\boldsymbol{k}$ is the deuteron momentum in the overall CMS, $\boldsymbol{q}$ denotes the K^+ momentum in the $K\bar{K}$ system, and $\hat{\boldsymbol{p}}$ is the unit vector of the beam momentum. Only $K\bar{K}$ p-waves contribute to C_0^q and C_2, only $K\bar{K}$ s-waves to C_0^k and C_1, and only s-p interference terms to C_3 and C_4. The coefficients C_i can be determined from the data by fitting Eq.(1) to the measured $\mathrm{d}\sigma/\mathrm{d}m_{K\bar{K}}$ and $\mathrm{d}\sigma/\mathrm{d}m_{dK}$ as well as to the angular distributions $\mathrm{d}\sigma/\mathrm{d}[\cos(\boldsymbol{pk})]$, $\mathrm{d}\sigma/\mathrm{d}[\cos(\boldsymbol{pq})]$, $\mathrm{d}\sigma/\mathrm{d}[\cos(\boldsymbol{kq})]$ and $\mathrm{d}\sigma/\mathrm{d}[\cos(\boldsymbol{pt})]$ [19] ($\boldsymbol{t}$ represents the K^+ momentum measured in the overall CMS). It should be noted that a fit to the two-dimensional Dalitz plot does not provide additional information about the transition matrix, but would only yield three linear combinations of two of the coefficients C_i [19].

$|\bar{\mathcal{M}}|^2$ gives the production probability of an event with certain kinematic parameters $\boldsymbol{k}$ and $\boldsymbol{q}$ relative to $\hat{\boldsymbol{p}}$. The corresponding differential acceptance of the spectrometer $\alpha(\boldsymbol{k},\boldsymbol{q},\hat{\boldsymbol{p}})$ does not depend on the values of C_i, and can be determined using a large sample of simulated events, covering full phase space, which are tracked through a GEANT model of the setup [27]. Using the coefficients from Ref. [21] as starting parameters, the simulations were carried out for different sets of the C_i, leading to differential distributions convoluted with the acceptance. For each choice of the C_i, the χ^2 values have been calculated for the difference between simulated and measured distributions. Subsequently, the coefficients which describe the experimental data best have been determined by minimizing χ^2 with the MINUIT package [28]. The best fit result of this procedure is shown in Fig. 3 for two invariant-mass and four angular distributions (cf. Table 1 in Sect. 3.1 for numerical values).

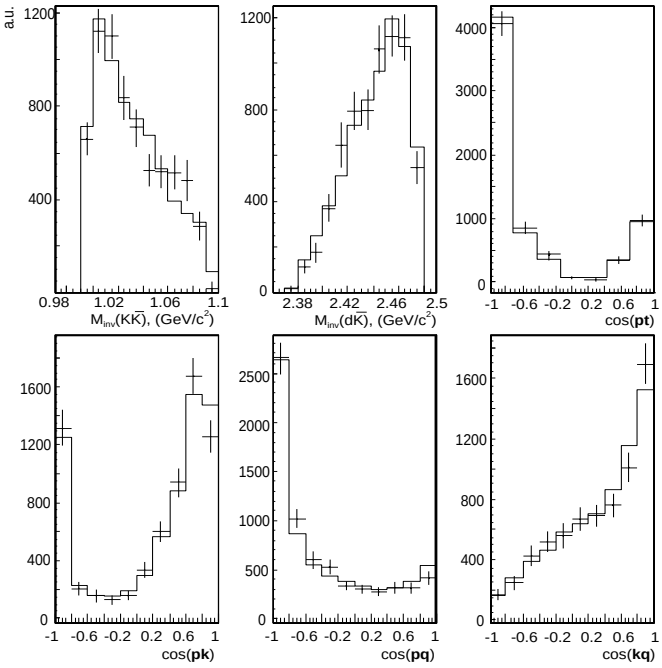

Fig. 3. Best fit to non-acceptance-corrected data at $T_p = 2.83$ GeV.

3 Cross sections of the reaction pp → $dK^+\bar{K}^0$ at Q = 47.4 and 104.7 MeV

3.1 Differential spectra

With the best fit coefficients C_i one can simulate corresponding differential distributions at the target, track the events through the setup, and thus determine one-dimensional differential acceptances for *e.g.* the two invariant masses and four angles of Fig. 3. Using these acceptances, differential cross sections can be extracted from the data, and these are shown in Fig. 4.

In order to verify the validity of the acceptance correction method using the coefficients C_i, the same procedure has been applied to the lower energy data. The results are shown in Fig. 5 as solid dots and are compared to our results published previously [21], analyzed using the acceptance matrix method (open circles). For a pp initial state all distributions must be forward-backward symmetric relative to the beam momentum; this feature has been exploited in Ref. [21], where differential cross sections as functions of $|\cos(\boldsymbol{pq})|$ and $|\cos(\boldsymbol{pk})|$ are presented. These are shown in the lower left spectra of Fig. 5 together with the mirrored distributions from the coefficient method (squares), each scaled by 0.25 for better distinction. In all cases good agreement between the model-independent matrix method [21] and the *ansatz* discussed here is observed. Note that the matrix method did not allow us to extract the $\cos(\boldsymbol{pt})$ distribution (upper right in the Figure) from the 2.65 GeV data which is now possible with the coefficient *ansatz*.

The best-fit coefficients C_i are presented in Table 1 for both beam energies. All coefficients are given in units

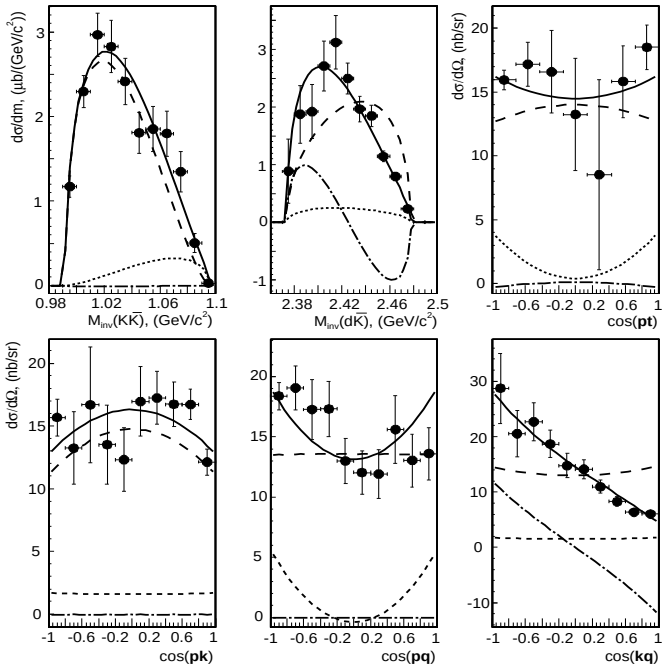

Fig. 4. Angular and invariant mass distributions for $T_p = 2.83$ GeV. The dashed (dotted) line corresponds to $K\bar{K}$ production in a relative s- (p-)wave, the dash-dotted to the interference term, and the solid line is the sum of these contributions. The error bars show the statistical uncertainties only. The systematic uncertainty for each bin is smaller than 10%; the overall uncertainty from the luminosity determination is given in Sect. 2.1.

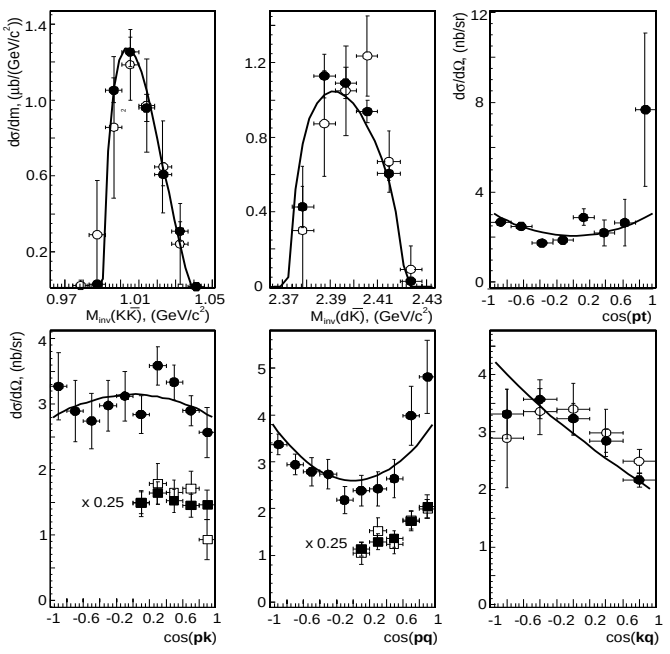

Fig. 5. Same as Fig. 4 for $T_p = 2.65$ GeV but omitting the fitted partial-wave contributions. Full symbols denote the differential cross sections obtained by the method described in this paper; open symbols are the previously published model-independent results [21] where the error bars include statistical and systematic uncertainties. The $\cos(\boldsymbol{pt})$ spectrum has not been presented in Ref. [21]. See text for further details.

of C_0^k. This is due to the fact that $|\bar{\mathcal{M}}|^2$ from Eq.(1) is proportional to the differential cross sections, thus leaving one parameter undetermined in the fit. The errors of the C_i are obtained by varying each coefficient (allowing the others to change) such that the total χ^2 increases by one.

The parameters C_i from Eq.(1) can be directly related to the different partial waves [21]. Their contributions to the various observables are shown in Fig. 4. The occurrence of interference terms in the $\bar{K}^0 d$ invariant mass distribution is due to the choice of the kinematic variables, *i.e.* relative momentum of the kaons and that of the deuteron with respect to the kaon pair. Consequently, there is no interference term in the $K^+\bar{K}^0$ mass distribution. To get a distribution for the other invariant mass that is free of interferences one needs to switch to the $\bar{K}^0 d$ relative momentum and the K^+ momentum. Then, however, there will be an interference term in the $K^+\bar{K}^0$ mass distribution. The method how to construct the variable transformation is described in detail in Ref. [29].

Our fit reveals a strong dominance of the $K\bar{K}$ s-wave production rate (*i.e.* via the $a_0^+(980)$ channel) for both beam energies: $(95 \pm 4)\%$ and $(89 \pm 4)\%$ at $T_p = 2.65$ GeV and 2.83 GeV, respectively.

The quality of the fit clearly supports the *ansatz* to include only the lowest partial waves in the data analysis. It should be noted that the growth of the amplitudes due to the centrifugal-barrier factor is taken care off by Eq.(1). An essential question is to understand the variation in the parameters C_3 and C_4, see Table 1. As outlined above, these parameters emerge solely from an interference of the $[(K\bar{K})_s d]_p$ with the $[(K\bar{K})_p d]_s$ partial waves. Therefore, if there were a significant phase motion in one of these groups (*e.g.* due to the strong final state interaction in the a_0 channel), a variation with energy especially of C_3 and C_4 is expected. This point clearly calls for more theoretical investigations.

3.2 Total cross sections

Knowing the coefficients C_i, and thus the initial differential distributions (Figs. 4 and 5), the total acceptance and the total cross sections can be evaluated. For the higher energy, a value of $\sigma(pp \to dK^+\bar{K}^0) = (190 \pm 4_{\rm stat} \pm 39_{\rm syst})$ nb is obtained. At the lower energy the extracted total cross section is in agreement with the previously published value of $(38 \pm 2_{\rm stat} \pm 14_{\rm syst})$ nb [21]. In both cases the errors include the statistical and systematic uncertainty from the luminosity determination.

Figure 6 shows the measured total cross sections in comparison with the expected Q dependence of the cross section calculated with the transition matrix element of Eq.(1). After an angular integration the total $pp \to dK^+\bar{K}^0$ cross section is given by

$$\sigma = \frac{N}{2^6\pi^3\sqrt{s^2 - 4sm_p^2}} \int\limits_{4m_K^2}^{(\sqrt{s}-m_d)^2} \frac{k\,q}{\sqrt{s}\;s_{KK}} \,|\tilde{\mathcal{M}}|^2 \;\mathrm{d}s_{KK} \;, \quad (2)$$

Table 1. Quality and results of the fit using Eq.(1). For the definition of N see Eq. 2.

Q, MeV	C_0^k	C_0^q	C_1	C_2	C_3	C_4	χ^2/ndf	N, μb MeV^{-2}
47.4	1	$-0.34^{+0.26}_{-0.21}$	$-0.14^{+0.14}_{-0.13}$	$1.23^{+0.32}_{-0.32}$	$-0.44^{+0.16}_{-0.16}$	$-0.76^{+0.30}_{-0.33}$	1.38	26.6 ± 10.9
104.7	1	$-0.07^{+0.14}_{-0.24}$	$-0.22^{+0.12}_{-0.11}$	$1.04^{+0.36}_{-0.19}$	$-1.45^{+0.20}_{-0.12}$	$0.09^{+0.25}_{-0.55}$	1.10	13.5 ± 3.0

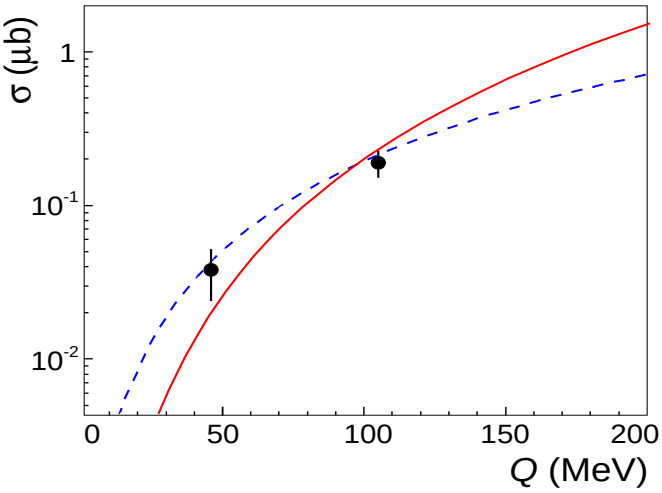

Fig. 6. Total cross section of the $pp \to dK^+\bar{K}^0$ reaction as function of the excess energy Q. The solid line is the result from Eq.(2) with the squared transition amplitude given by Eq.(3) and with N=18 μb MeV^{-2}. The dashed line shows the energy dependence for three-body phase space. Note that the latter is forbidden by selection rules.

where s and s_{KK} are the squared invariant energies of the initial pp and final $K^+\bar{K}^0$ systems, respectively. Here k and q are defined as before and are given explicitly as

$$k^2 = \frac{(s - s_{KK} - m_d^2)^2 - 4 s_{KK} m_d^2}{4s},$$
$$q^2 = \frac{s_{KK} - 4m_K^2}{4},$$

where m_d and m_K are the deuteron and kaon masses, *i.e.* we neglect the K^+ and $\bar{K}^0$ mass difference. The angular-integrated squared transition amplitude $|\tilde{\mathcal{M}}|^2$ is given as

$$|\tilde{\mathcal{M}}|^2 = \left(C_0^q + \frac{1}{3}C_2\right) q^2 + \left(C_0^k + \frac{1}{3}C_1\right) k^2. \qquad (3)$$

The normalization factor N has been determined for both energies and is quoted in Table 1. The errors of N include the systematic uncertainties of the total cross sections. Note that the lines in Figs. 4 and 5 have been properly scaled to the individual total cross sections.

For illustration we show by the dashed line in Fig. 6 the result of Eq.(2) with a constant matrix element. This is a classical example when data can be well reproduced by a simple phase-space consideration although such a description is invalid for this particular reaction since selection rules do not allow for a pure s-wave.

4 Summary and conclusions

Using the ANKE spectrometer at an internal target position of COSY-Jülich, we have searched for scalar $K\bar{K}$ production in the reaction $pp \to dK^+\bar{K}^0$ at two excess energies Q = 47.4 and 104.7 MeV. Due to the excellent K^+ identification at ANKE, the detected events with coincident K^+d pairs exhibit little background. This can be subtracted using events outside the $\bar{K}^0$ missing-mass peak. After a kinematic fit to the $\bar{K}^0$ mass, the invariant $K^+\bar{K}^0$ mass distribution has been obtained with an unprecedented resolution of better than 3 (10) MeV/c^2 for 47.4 (104.7) MeV.

Mass and angular distributions have been extracted from the data using an *ansatz* for the transition matrix element that includes the lowest allowed partial waves, *i.e.* an s-wave in the $K\bar{K}$ system accompanied by a p-wave of the deuteron with respect to the meson pair and p-wave $K\bar{K}$ production with an s-wave deuteron. All six coefficients that enter the spin-averaged matrix element have been obtained by a fit to the differential spectra. This fit reveals the dominance of $K\bar{K}$ production in a relative s-wave, (95 ± 4)% and (89 ± 4)% at 47.4 and 104.7 MeV, *i.e.* dominance of kaon-pair production via the $a_0^+(980)$ channel.

The reaction $pp \to dK^+\bar{K}^0$ has been subject of several theoretical papers. For example, the authors of Ref. [30] point out that this reaction (and also $pp \to d\pi^+\eta$) is expected to be an additional source of information about the scalar sector. They account for the interactions of the mesons by using chiral unitary techniques, which dynamically generate the $a_0^+(980)$ resonance. In Ref. [31] total cross sections and differential spectra are calculated using a model in which the reaction $pp \to dK^+\bar{K}^0$ is dominated by intermediate $a_0^+(980)$ production.

As discussed in Sect. 3.1, there is an energy dependence of the parameters C_3 and C_4 in the transition matrix element (Eq.(1)) that is not yet understood and needs further theoretical study since it might indicate a final-state interaction in the a_0 channel.

Acknowledgements

This work has been carried out within the framework of the ANKE Collaboration [32] and supported by the COSY-FFE program, the Deutsche Forschungsgemeinschaft (436 RUS 113/337, 444, 561, 768, 787), Russian Academy of Sciences (02-04-034, 02-04034, 02-18179a, 02-06518, 02-16349). We are grateful to the COSY-accelerator crew for providing the proton beam above the nominal accelerator

energy. Special thanks to C. Wilkin for carefully reading the manuscript and for conducting photomultiplier tests.

References

1. T. Kunihiro *et al.* [SCALAR Collaboration], Phys. Rev. D **70**, 034504 (2004).
2. D. Morgan, Phys. Lett. B **51**, 71 (1974); K.L. Au, D. Morgan, and M.R. Pennington, Phys. Rev. D **35**, 1633 (1987); D. Morgan and M.R. Pennington, Phys. Lett. B **258**, 444 (1991); D. Morgan and M.R. Pennington, Phys. Rev. D **48**, 1185 (1993); A.V. Anisovich *et al.*, Eur. Phys. J. A **12**, 103 (2001); S. Narison, hep-ph/0012235.
3. S. Eidelman *et al.* (Particle Data Group); Phys. Lett. B **592**, 1 (2004).
4. J. Weinstein and N. Isgur, Phys. Rev. Lett. **48**, 659 (1982); Phys. Rev. D **27**, 588 (1983); Phys. Rev. D **41**, 2236 (1990); G. Janssen *et al.*, Phys. Rev. D **52**, 2690 (1995); J.A. Oller and E. Oset, Nucl. Phys. A **620**, 438 (1997) [Erratum-ibid. A **652**, 407 (1999)].
5. N.N. Achasov, hep-ph/0201299; R.J. Jaffe, Phys. Rev. D **15**, 267 (1977); J. Vijande *et al.*, Proc. Int. Workshop MESON 2002, May 24–28, 2002, Cracow, Poland, World Scientific Publishing, ISBN 981-238-160-0, p.501, hep-ph/0206263.
6. F.E. Close and N.A. Törnqvist, J. Phys. G **28**, R249 (2002).
7. J.B. Gay *et al.*, Phys. Lett. B **63**, 220 (1976).
8. A. Abele *et al.*, Phys. Lett. B **327**, 425 (1994); A. Abele *et al.*, Phys. Rev. D **57**, 3860 (1998); A. Bertin *et al.*, Phys. Lett. B **434**, 180 (1998).
9. S. Teige *et al.*, Phys. Rev. D **59**, 012001 (1999).
10. P. Achard *et al.*, Phys. Lett. B **526**, 269 (2002).
11. N.N. Achasov *et al.*, Phys. Lett. B **485**, 349 (2000); Phys. Lett. B **479**, 53 (2000).
12. A. Aloisio *et al.*, Phys. Lett. B **536**, 209 (2002); Phys. Lett. B **537**, 21 (2002).
13. D. Barberis *et al.*, Phys. Lett. B **440**, 225 (1998); Phys. Lett. B **488**, 225 (2000).
14. M.A. Abolins *et al.*, Phys. Rev. Lett. **25**, 469 (1970).
15. V. Baru *et al.*, Phys. Lett. B **586**, 53 (2004).
16. V. Baru *et al.*, Eur. Phys. J. A **23**, 523 (2005).
17. R. Maier, Nucl. Instr. and Methods Phys. Res., Sect. A **390**, 1 (1997).
18. M. Büscher, Acta Phys. Pol. B **35**, 1055 (2004).
19. C. Hanhart, Phys. Rept. **397**, 155 (2004).
20. N.N. Achasov *et al.*, Phys. Lett. B **88**, 367 (1979).
21. V. Kleber *et al.*, Phys. Rev. Lett. **91**, 172304 (2003).
22. P. Fedorets *et al.*, Phys. Atom. Nucl. [Yad. Fiz.] **69**, 306 (2006).
23. S. Barsov *et al.*, Nucl. Instr. and Methods Phys. Res., Sect. A **462**, 364 (2001).
24. R. Santo *et al.*, Nucl. Instr. and Methods Phys. Res., Sect. A **386**, 228 (1997); A. Khoukaz *et al.*, Eur. Phys. J. D **5**, 275 (1999).
25. M. Büscher *et al.*, Nucl. Instr. and Methods Phys. Res., Sect. A **481**, 378 (2002).
26. S. Dymov *et al.*, Phys. Lett. B **635** 270 (2006).
27. I. Zychor, Acta Phys. Pol. B **33**, 521 (2002).
28. F. James and M. Roos, Comput. Phys. Commun. **10**, 343 (1975).
29. A. Sibirtsev, M. Büscher, V. Y. Grishina, C. Hanhart, L. A. Kondratyuk, S. Krewald and U. G. Meissner, Phys. Lett. B **601** (2004) 132.
30. E. Oset, J. A. Oller and U.-G. Meissner, Eur. Phys. J. A **12** (2001) 435.
31. V. Y. Grishina *et al.*, Eur. Phys. J. A **21**, 507 (2004).
32. The ANKE Collaboration: `www.fz-juelich.de/ikp/anke`.